Comparison of microwave-induced combustion and solid-state reaction method for synthesis of $LiMn_{2-x}Co_xO_4$ powders and their electrochemical properties

YEN-PEI FU*
Department of Materials Science and Engineering, National Dong-Hwa University, Shou-Feng, Hualien, 974 Taiwan
E-mail: ypfu@mail.ndhu.edu.tw

YU-HSIU SU
Department of Materials Science and Engineering, National Tsing-Hua University, Hsinchu, 300 Taiwan

CHENG-HSIUNG LIN
Department of Chemical Engineering, Wu-Feng Institute of Technology, Ming-Hsiung, Chiayi, 621 Taiwan

SHE-HUANG WU
Department of Materials Engineering, Ta-Tung University, Taipei, 104 Taiwan

Published online: 28 February 2006

Spinel $LiMn_{2-x}Co_xO_4$ ($0.00 \leqq x \leqq 0.20$) powders with small and uniform particle size were successfully synthesized by microwave-induced combustion using lithium nitrate, manganese nitrate, cobalt nitrate, and urea as the starting materials. The $LiMn_{2-x}Co_xO_4$ powders synthesized by microwave-induced combustion were investigated by X-ray diffractometer (XRD), thermogravimeter analyzer (TG), and scanning electron microscopy (SEM). The $LiMn_{2-x}Co_xO_4$ samples were used as cathode materials in lithium-ion batteries, whose discharge capacity and electrochemical characteristics such as the cycling performance were also investigated. The results revealed that the $LiMn_{2-x}Co_xO_4$ cell synthesized by microwave-induced combustion provided a high initial capacity and excellent reversibility compared to the material prepared by solid-state reaction method.

1. Introduction

Spinel-type $LiMn_2O_4$ has recently become an attractive material for making the cathode of lithium-ion rechargeable batteries because of its relative low cost and high capacity [1–3]. However, the capacity of $LiMn_2O_4$ fades during cycling for several reasons, such as an instability of an organic-base electrolyte operated in a high potential region [4], the dissolution of manganese into the electrolyte [5, 6], changes in crystal lattice arrangement with cycling [7] and others. The manganese ion has been partially replaced by other transition metal ions, such as Ni, Cr, and Co to improve capacity fading [8–10]. The conventional way to produce these materialsis prepared by the solid-state reaction of mixtures of oxides or carbonates containing lithium and manganese cations, those are calcined at high temperatures. However, the solid-state reaction requires a long heating time followed by several grinding and an annealing processes, which has some inherent disadvantages such as chemical inhomogeneity, coarser particle size, and introduction of impurities during ball milling. Several chemical methods such as co-precipitation, sol-gel, Pechini, and ultrasonic spray pyrolysis have been developed to overcome the above-mentioned disadvantages, which synthesized by

*Author to whom all correspondence should be addressed.
0022-2461
DOI: 10.1007/s10853-005-3646-4

solid-state reaction. However, these chemical methods involve complicated steps such as precise control of pH, precipitation, etc., to obtain the correct stoichiometric compound.

This work employs a new method called microwave-induced combustion synthesis to produce a series of Co-doped $LiMn_{2-x}Co_xO_4$ powders. Microwave processing of materials is fundamentally different from the conventional processing in terms of the heat generation mechanism. In a microwave oven, heat is generated within the sample itself by the interaction of microwaves with the material. Conventional heating generates heat by heating elements; the heat is then transferred to the sample surfaces [11]. The microwave-induced combustion synthesis entails the dissolution of lithium nitrate, manganese nitrate, cobalt nitrate, and urea in water, and then heating the resulting solution in a microwave oven. Urea and metal nitrate decompose giving off flammable gases such as NH_3, HNCO, and NO. After the solution reaches the point of spontaneous combustion, it begins to burn in a solid form above 1000°C. The combustion is not complete until all the flammable substances are all burnt out. The product is a loose substance, which shows voids, pores and is a highly friable material, formed by the escaping gases during the combustion reaction [12]. The whole process takes only 30 min to yield $LiMn_{2-x}Co_xO_4$ powders.

In this study, a series of Co-doped $LiMn_{2-x}Co_xO_4$ powders prepared by microwave-induced combustion in comparison to materials prepared by solid–state reaction have been investigated. Moreover, the capacity and reversible performance of the Li/$LiMn_{2-x}Co_xO_4$ cells have also been examined.

2. Experiment procedure

2.1. Preparation of $LiMn_{2-x}Co_xO_4$ powders

2.1.1. Microwave-induced combustion

The synthesis process of $LiMn_{2-x}Co_xO_4$ powders involved the combustion of redox mixtures, in which metal nitrates act as oxidizing agents and the urea as a reducing agent. The initial composition of the solution containing lithium nitrate, manganese nitrate, cobalt nitrate, and urea was based on the total oxidizing and reducing capability of the oxidizer and fuel using the concepts of propellant chemistry. The stoichiometry of the redox mixtures used for combustion was determined using the total oxidizing and reducing properties of the components which serve as numerical coefficients for the stoichmetric balance so that the equivalence ratio (Φ_e) is unity and the energy released by combustion is a maximum. According to this concept, the valences of some elements and ions are as follows: C = +4, H = +1, O = −2, divalent metal ions = −2, and trivalent metal ions = −3. The valence of nitrogen is considered to be zero. Accordingly, the oxidizing and reducing properties of the compounds used in the combustion mixtures can be calculated [13].

Stoichiometric amounts of lithium nitrate [$LiNO_3$] 1.5 M, the total concentration of manganese nitrate [$Mn(NO_3)_2{\cdot}6H_2O$] and cobalt nitrate [$Co(NO_3)_2{\cdot}6H_2O$] was 3.0 M. The atomic ratios of (Mn+Co)/Li were set to be 2. The amount of urea, which corresponds to a ratio of fuel to nitrate in which the fuel can react completely with the nitrates, was calculated by the concepts of propellant chemistry. The solution contained with urea and nitrates were poured into a crucible with 15 ml. Then, the crucible was placed in a microwave oven (CEM, MDS 81D, 650W). The microwave power of microwave oven operated at 100% (650 W) for 30 min. Initially, the solution boiled and underwent dehydration followed by materials decomposition with the evolution of large amount of gases (N_2, NH_3, and HNCO). After the system reached the point of spontaneous combustion, it began to burn with the release of much heat and vaporized all of the liquid instantly. The entire combustion process for producing $LiMn_{2-x}Co_xO_4$ powders in the microwave oven took only 30 min, and then the microwave-heated $LiMn_{2-x}Co_xO_4$ powders were annealed at the temperature of 800°C for 8 h in air, followed by controlled cooling to room temperature at about 2°C/min.

2.1.2. Solid state reaction

The $LiMn_{2-x}Co_xO_4$ ($0.00 \leqq x \leqq 0.20$) powders were prepared by the solid-state reaction from a stoichiometric mixture of $LiCO_3$, $MnCO_3$, and CoO. The mixtures were preheated at 800°C for 8 h and ground after cooling, then heated at 800°C for 24 h in air, followed by controlled cooling to room temperature at about 2°C/min.

2.2. Characterization

The crystallography of samples were characterized using a computer-interface X-ray powder diffractometer (XRD; Rigaku D/Max-II) with Cu K_α radiation. The lattice constants were calculated by an iterative least square refinements method using 10 wt% silicon as an internal standard. The particle morphology and size of the microwave-heated $LiMn_{2-x}Co_xO_4$ powders and that were annealed at 800°C for 8 h were characterized using scanning electron microscopy (SEM; JEOL JSM-6500F). The thermal decomposition behavior of $LiMn_2O_4$ powders of the as-prepared microwave-induced combustion and solid-state reaction were analyzed by means of thermogravimetry (TG; Rigaku Thermalplus TG 8120). A heating rate of 10°C/min from room temperature up to 1000°C was obtained under flowing dry air.

The charge and discharge characteristics of $LiMn_{2-x}Co_xO_4$ cathode materials were examined in laboratory cells. The cells consist of a cathode and a lithium metal anode and a micro-porous polypropylene separator. The electrolyte was 1M $LiPF_6$ in a 50/50 vol% solvent of EC/DMC. The positive electrode consisted of a mixture of 83 wt% of cathode material, 10 wt% of actylene black, and 7 wt% poly vinylidene flouoride

(PVDF). The mixture was pressed onto a stainless screen mesh at 250 kg/cm^2 and vacuum dried at 110°C for 12 h in a oven. The cells were cycled at room temperature in the voltage range of 3.0–4.5 V vs. Li/Li$^+$ with a typical current density 0.1 mA/cm^2. Cyclic voltammetry was performed for the cathode materials using a flooded three-electrode glass cell. The cyclic voltamograms were taken at a sweep rate of 0.05 mV/s between 3.0–4.5 V vs. Li/Li$^+$. Assembly of the cell was carried out in a glove box filled with Ar gas.

3. Results and discussion

3.1. Properties of synthesized powders

Phase transformation of microwave-heated $LiMn_2O_4$ powders and the mixtures of the reactants $LiCO_3$ with $MnCO_3$ powders were studied using TG measurement. Fig. 1a shows the TG curve for the mixtures of the reactants $LiCO_3$ with $MnCO_3$ powders (atomic ratios of Mn/Li were set to be 2). There are three heat steps for the weight loss. The first step from room temperature to 200°C may be attributed to the evaporation of residual water; whereas the second step between 250–420°C is due to nitrate and urea decomposition and followed by the crystallization of $LiMn_2O_4$ phase; the third step above 450–900°C, which indicates the weight loss of mixtures is about 3%. The latter weight loss was due to the solid-state reaction completed the formation of $LiMn_2O_4$ at this stage. Fig. 1b shows the TG trace for microwave-heated $LiMn_2O_4$ powders, which indicates the weight loss is about 5% during the whole heating process. This can be attributed to the fact that mainly all the $LiMn_2O_4$ spinel phase had been formed during the microwave-induced combustion process. Microwaves force unpaired electrons to oscillate between the vacant lattice sites, causing an intramolecular friction between the Mn and Li ions. This friction generates sufficient heat to promote the spinel formation if the necessary ingredients are present.

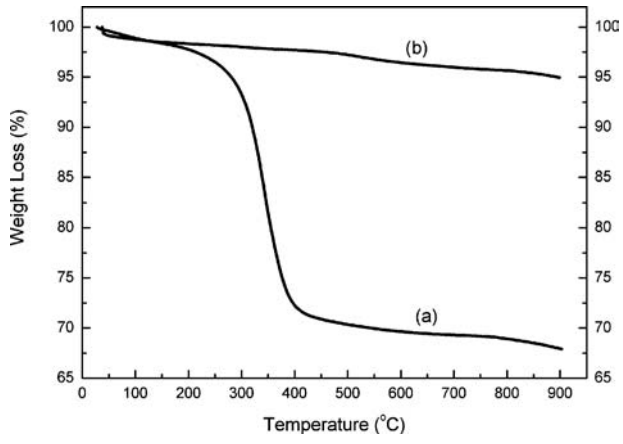

Figure 1 The thermogravimetric analysis curves for (a) the mixtures of the reactants $LiCO_3$ with $MnCO_3$ powders, (b) the microwave-heated $LiMn_2O_4$ powders.

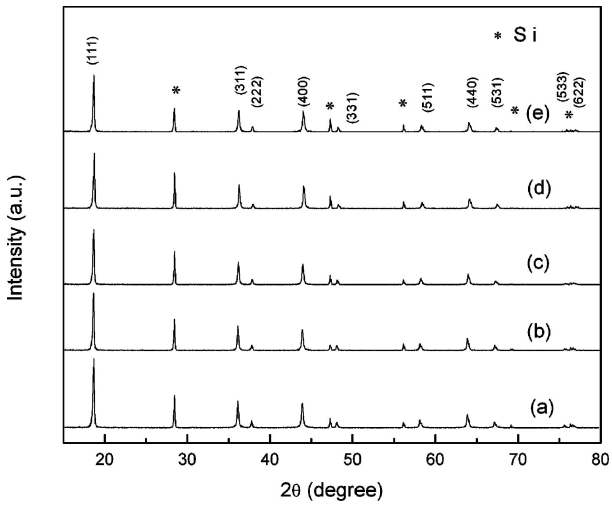

Figure 2 XRD patterns of spinel $LiMn_{2-x}Co_xO_4$ powders for (a) $x = 0$, (b) $x = 0.05$, (c) $x = 0.10$, (d) $x = 0.15$, and (g) $x = 0.20$ prepared by microwave-induced combustion and annealing at 800°C for 8 h.

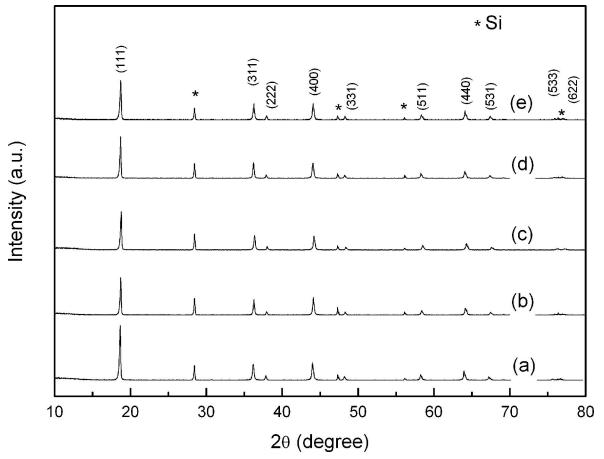

Figure 3 XRD patterns of spinel $LiMn_{2-x}Co_xO_4$ powders for (a) $x = 0$, (b) $x = 0.05$, (c) $x = 0.10$, (d) $x = 0.15$, and (e) $x = 0.20$ prepared by solid-state reaction. The mixtures were preheated at 800°C for 8 h and finally heated at 800°C for 24 h in air.

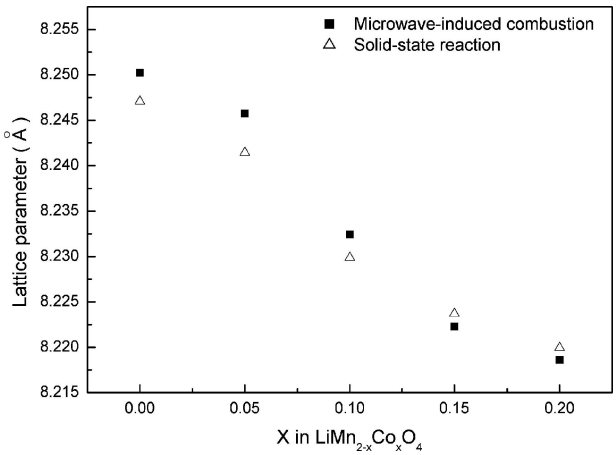

Figure 4 The lattice parameter of $LiMn_{2-x}Co_xO_4$ powders synthesized by microwave-induced combustion and solid-state reaction.

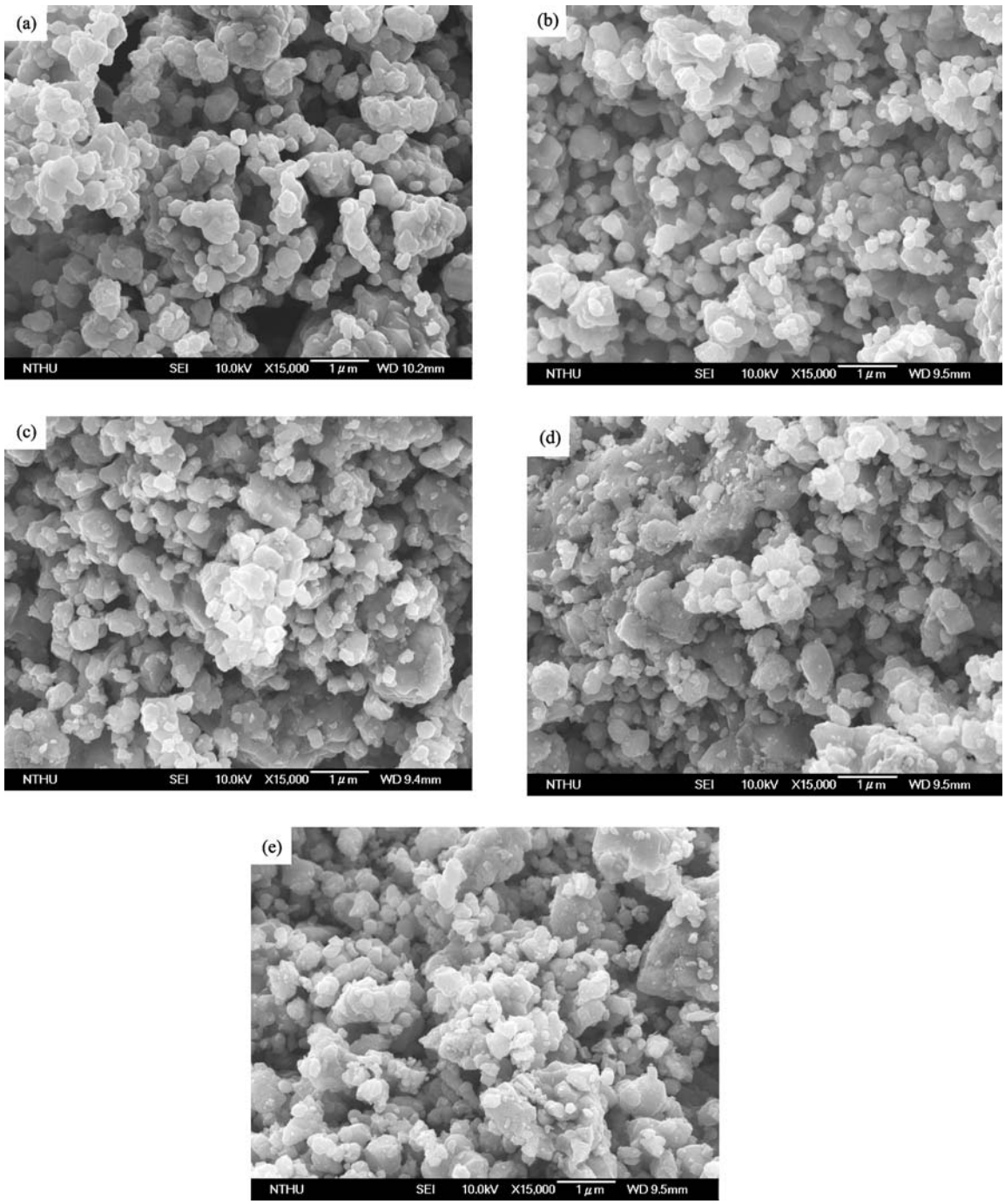

Figure 5 SEM photographs of the microwave-heated $LiMn_{2-x}Co_xO_4$ powders: (a) $x = 0$, (b) $x = 0.05$, (c) $x = 0.10$, (d) $x = 0.15$, and (e) $x = 0.20$ annealed at 800°C for 8 h.

Fig. 2 shows the X-ray diffraction patterns of the microwave-heated $LiMn_{2-x}Co_xO_4$ ($0.00 \leqq x \leqq 0.20$) powders that was annealed at 800°C for 8 h. Evidently, the microwave-heated $LiMn_{2-x}Co_xO_4$ powders annealed at 800°C for 8 h contained only a single phase of cubic spinel with a space group Fd3m, where lithium ions occupy the tetrahedral sites (8a); Mn^{3+} and Mn^{4+} ions reside at the octahedral sites (16d); and O^{2-} ions are located at 32e sites. The XRD patterns of $LiMn_{2-x}Co_xO_4$ powders did not differ with the various compositions. Such excellent structure should provide excellent performance for $Li/LiMn_{2-x}Co_xO_4$ cells. On the other hand, similar XRD results were also observed in solid-state reaction (Fig. 3). The XRD result indicates that microwave-induced combustion method could synthesize a pure $LiMn_2O_4$ phase in a shorter time than the solid-state reaction.

The variation in lattice parameter as a function of x values for $LiMn_{2-x}Co_xO_4$ powders synthesized by microwave-induced combustion and solid-state reaction are plotted in Fig. 4. It can be clearly observed that the

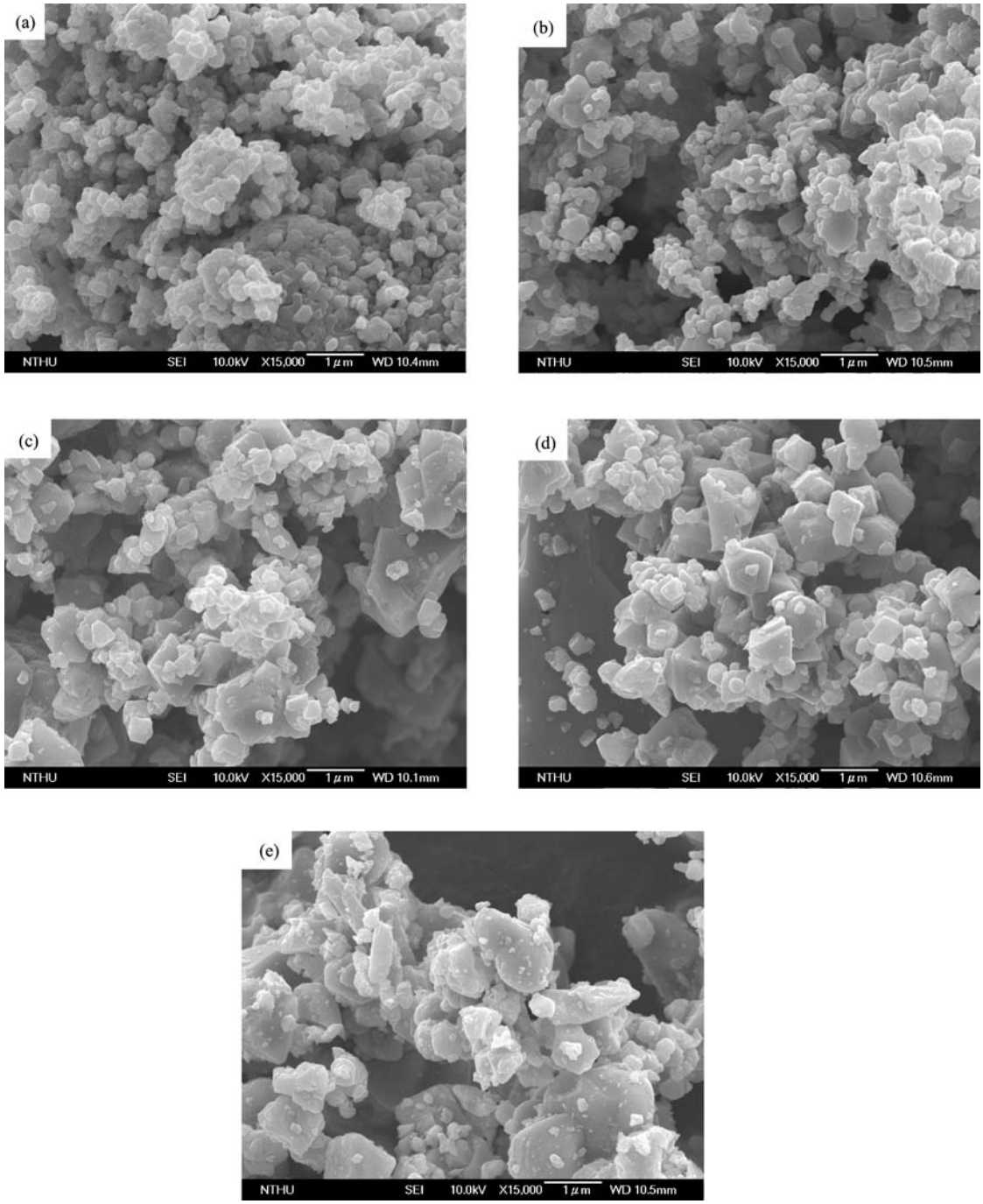

Figure 6 SEM photographs of $LiMn_{2-x}Co_xO_4$ powders: (a) $x = 0$, (b) $x = 0.05$, (c) $x = 0.10$, (d) $x = 0.15$, and (e) $x = 0.20$ synthesized by solid-state reaction.

lattice constant decreases as x values increase from 0.00 to 0.20. This was due to substituted spinel phase; the Mn–Mn and Mn–O interatomic distances decreased with the increasing Co content. It also implied that the average valence of Mn ion increased with increasing Co content. This was ascribed to the Mn^{3+} ions that were substituted by Co^{3+}. Therefore, a slightly lower Mn^{3+} content and higher Mn^{4+} content were presented in the Co-substituted spinel samples. This behavior will suppress the Jahn-Teller distortion for $Li/LiMn_{2-x}Co_xO_4$ cells after many cycles of charge and discharge. Notably, as the Co content is increased to more than 0.15 mol, the $LiMn_{2-x}Co_xO_4$ powders synthesized by microwave-induced combustion possessed higher lattice parameters than those synthesized by solid-state reaction. It suggests that $Li/LiMn_{2-x}Co_xO_4$ cells prepared by microwave-induced method had better cycling performance than those prepared by solid-state reaction, as the Co content increased to more than 0.15 mol.

Since the particle size is an important factor for cycling performance of the $Li/LiMn_{2-x}Co_xO_4$ cells, particle morphology and particle size were examined by scanning electron microscopy. Fig. 5 presents micrographs of

the microwave-heated $LiMn_{2-x}Co_xO_4$ powders with various x values annealed at 800°C for 8 h. As shown in Fig. 5a–d, the microwave-heated $LiMn_{2-x}Co_xO_4$ powder with x value from 0.00 to 0.15 have a uniform particle size range of 0.5 to 0.8 μm. Fig. 5e, the microwave-heated $LiMn_{2-x}Co_xO_4$ powders with $x = 0.20$, have a broad particle distribution and forms some particle agglomerates. On the other hand, the variation of particle size and morphology of $LiMn_{2-x}Co_xO_4$ powders prepared by solid-state reaction are shown in Fig. 6. According to SEM observation, we observed the following conclusions: The particle morphology of $LiMn_{2-x}Co_xO_4$ powders prepared by microwave-induced combustion revealed a planar-lamination shape. In contrast, those powder prepared by solid-state reaction exhibited a polyhedral morphology.

3.2. Electrochemical properties

The performance of $LiMn_{2-x}Co_xO_4$ as the cathode of the lithium-ion battery was examined as follows. Fig. 7 shows the cyclic voltammogram for $LiMn_{2-x}Co_xO_4$ cells synthesized by microwave-induced combustion with $x =$ 0.00, 0.10, and 0.20 at a sweep rate of 0.05 mV/s. The current-voltage curve clearly demonstrated the reversibility of this material upon deintercalation and intercalation of Li^+ over the range of 3.0 to 4.5 V vs. Li/Li^+. Clearly, all the samples revealed two pairs of redox peaks in the cyclic voltammogram, indicating lithium ions are extracted and inserted into spinel $LiMn_{2-x}Co_xO_4$ in a two-step process. The presence of two pairs may be ascribed to the fact that lithium ions are removed from half the tetrahedral sites, in which Li-Li interactions occur, and than lithium ions are removed from the other tetrahedral sites in which lithium ions do not have nearest neighbor Li-Li interactions [14]. Moreover, the two characteristic peaks of the spinel can be distinguished by their small amount of Co content, which also suggest that a small amount of

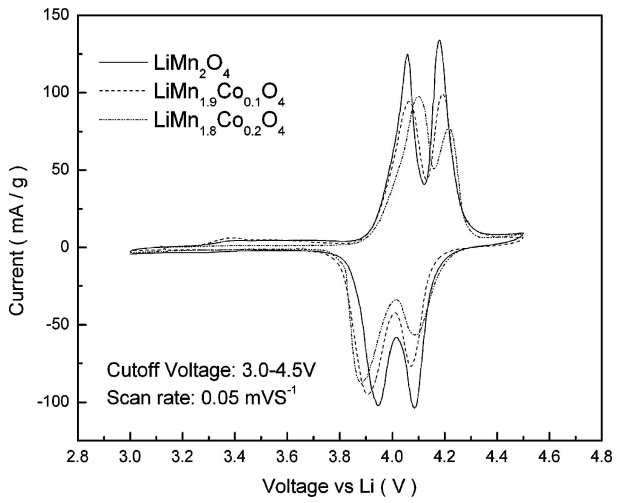

Figure 7 Cyclic voltammogram over the potential 3.0–4.5 V for $LiMn_2O_4$, $LiMn_{-1.9}Co_{0.1}O_4$, and $LiMn_{1.8}Co_{0.2}O_4$ at a scan rate of 0.05 mV/s.

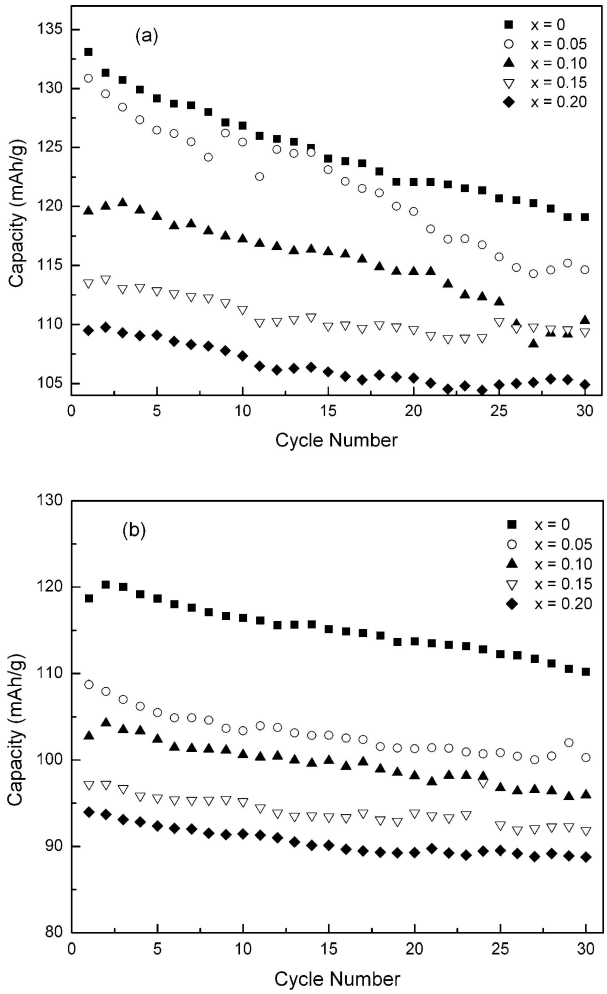

Figure 8 Relationships between the capacity and cycle number of the $Li/LiMn_{2-x}Co_xO_4$ cells prepared by (a) microwave-induced combustion and (b) solid-state reaction.

Co does not disturb the spinel structure because of the ionic radii of Co^{3+} (0.065 nm) is slightly smaller than Mn^{3+} (0.070 nm). This crystal structure was consistent with XRD results. For the $Li/LiMn_2O_4$ cell, two anodic peaks were observed at 4.09 and 4.18 V. However, for the $Li/LiMn_{2-x}Co_xO_4$ cells with $x = 0.10$ and 0.20, the anodic peaks are smaller, broader, and shifted toward higher potentials. As depicted in Fig. 7, an increase in Co concentrations causes the peaks to merge into one, indicating the stability of the $Li/LiMn_{2-x}Co_xO_4$ cells was higher and the fading capacity was slower than those of pure spinel $Li/LiMn_2O_4$.

Fig. 8 plots the relationships between the discharge capacity at room temperature and the number of cycles for the $Li/LiMn_{2-x}Co_xO_4$ cells at a current rate of 0.1 mA between 3.0 to 4.5 V. The discharge capacity as function of cycle number for $Li/LiMn_{2-x}Co_xO_4$ cells prepared by microwave-induced combustion is plotted in Fig. 8a. On the other hand, the discharge capacity as function of cycle number for $Li/LiMn_{2-x}Co_xO_4$ cells prepared by solid-state reaction is plotted in Fig. 8b. As can be seen in both methods, with increasing Co content in $Li/LiMn_{2-x}Co_xO_4$ cells from $x = 0.00$ to $x = 0.20$, the

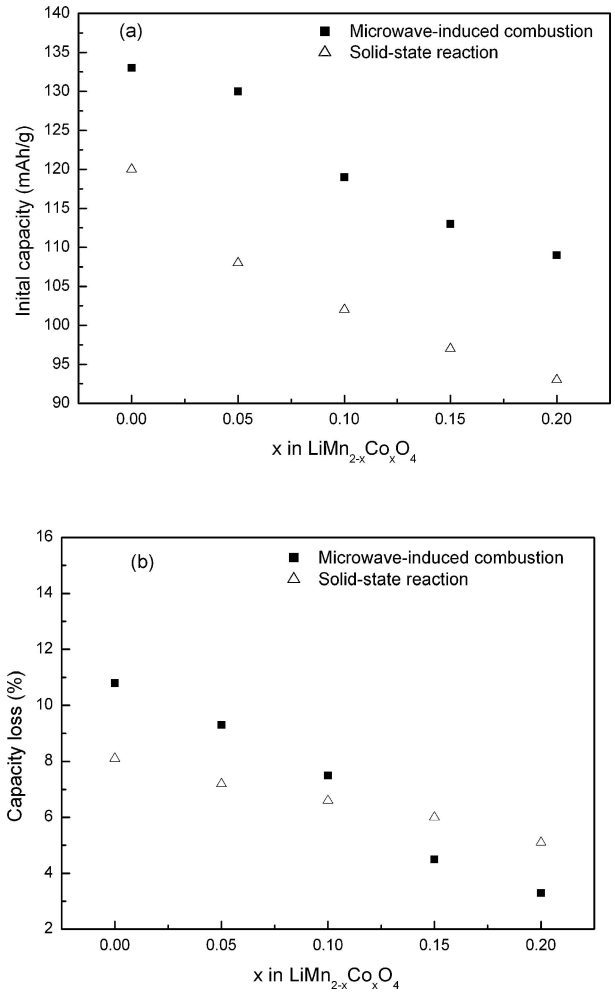

Figure 9 (a) Initial capacity and (b) capacity loss per cycle as function of Co content in Li/$LiMn_{2-x}Co_xO_4$ cells prepared by microwave-induced combustion and solid-state reaction.

initial capacity decreased gradually, primarily owing to Mn ion dissolution from spinel during cycling.

In order to further study the initial capacity and capacity loss of Li/$LiMn_{2-x}Co_xO_4$ cells, we summarized the relation of the initial capacity and capacity loss for Li/$LiMn_{2-x}Co_xO_4$ cells in Fig. 9. Fig. 9a shows the initial capacity of Li/$LiMn_{2-x}Co_xO_4$ cells prepared by microwave-induced combustion and solid-state reaction as a function of Co content. For the Li/$LiMn_{2-x}Co_xO_4$ cells prepared by microwave-induced combustion, the initial discharge capacity went from 133 to 109 mAh/g, as Co content increased went from $x = 0.00$ to 0.20. On the other hand, material prepared by solid-state reaction, had an initial discharge capacity of 118 that decreased to 93 mAh/g, as the Co content increased from $x = 0.00$ to 0.20.

The capacity loss per cycle was calculated by averaging the capacity loss over the first thirty cycles, where capacity loss can be define as $\frac{C_1 - C_n}{C_1} \times 100\%$, where C_1 and C_n are the discharge capacity of first and nth cycle, n is the number of cycles. The discharge capacity fading of the Li/$LiMn_{2-x}Co_xO_4$ cells after 30 cycles, which were prepared with materials from microwave-induced combustion and solid-state reaction is shown in Fig. 9b. It indicated that the Li/$LiMn_{2-x}Co_xO_4$ cells with $x = 0.20$ prepared by microwave-induced combustion, had a capacity loss a minimum of about 3.3%/cycle. This is ascribed to the fact that Co-doping suppresses the Jahn-Teller distortion in the spinel structure. In addition, the bonding energy of Co–O (1067 kJ/mol) is stronger than that of the Mn–O (946 kJ/mol) bond, which results in the greater stability of the spinel structure and decreases the capacity loss of the Li/$LiMn_{2-x}Co_xO_4$ cells after many cycles.

In Fig. 9b, as $0.00 \leqq x \leqq 0.10$, the capacity loss of the Li/$LiMn_{2-x}Co_xO_4$ cells prepared by solid-state reaction obtained a lower capacity loss than that prepared by microwave-induced combustion, whereas with the $0.15 \leqq x \leqq 0.20$ materials, the capacity loss of the Li/$LiMn_{2-x}Co_xO_4$ cells prepared by microwave-induced combustion shows lower capacity loss than that prepared by solid state reaction. This result is consistent with lattice parameter results (Fig. 4). This is ascribed to the fact that the average valence of Mn ion for microwave-induced combustion method is larger than solid-state reaction, it will suppress the Jahn-Teller distortion for Li/$LiMn_{2-x}Co_xO_4$ materials and improve the cycling performance during many cycles.

4. Conclusions

Using lithium nitrate, manganese nitrate, cobalt nitrate, and urea as the starting materials, uniform $LiMn_{2-x}Co_xO_4$ powders were synthesized successfully by microwave-induced combustion. The results revealed that spinel $LiMn_{2-x}Co_xO_4$ powders can be obtained by the microwave-induced combustion method in a short time compared with the solid-state reaction method; moreover the initial discharge capacity and cycling performance were better than those prepared by solid-state reaction.

Acknowledgment

The authors gratefully acknowledge the financial support from the National Science Council of the Republic of China under project no. NSC 93-2622-E-259-004-CC3.

References

1. S. KOMABA, K. OIKAWA, S.-T. MYUNG, N. KUMAGAI and T. KAMIYANA, *Solid State Ionics* **149** (2002) 47.
2. D. SONG, H. IKUTA, T. UCHIDA and M. WAKIHARA, *ibid.* **117** (1999) 151.
3. L. ZHANG, H. NOGUCHI and M. YOSHIO, *J. Power Sources* **110** (2002) 57.
4. R. J. GUMMOW, A. DE KOCK and M. WAKIHARA, *Solid State Ionics* **69** (1994) 59.
5. Y. XIA, Y. ZHOU and M. YOSHIO, *J. Electrochem. Soc.* **144** (1997) 2593.
6. S.-T. MYUNG, S. KOMABA and N. KUMAGAI, *Ibid.* **148** (2001) A482.
7. P. ARORA, B. N. POPOV and R. E. WHITE, *ibid.* **145** (1998) 807.

8. L. GUOHUA, H. IKUTA, T. UCHIDA and M. WAKIHARA, *ibid.* **143** (1996) 178.
9. K. AMINE, H. TUKAMOTO, H. YASUDA and Y. FUJITA, *J. Power Sources* **68** (1997) 604.
10. B. BANOV, Y. TODOROV, A. TRIFONOVA, A. MOMCHILOV and V. MANEV, *ibid.* **68** (1997) 578.
11. D. E. CLARK and W. H. SUTTON, *Ann. Rev. Mater. Sci.* **26** (1996) 299.
12. O. A. LOPEZ, J. MCKITTRICK and L. E. SHEA, *J. Lumin.* **71** (1997) 1.
13. S. R. JAIN, K. C. ADIGA and V. R. VERNEKER, *Comb. Flam.* **40** (1981) 71
14. Y. XIA and M. YOSHIO, *J. Electrochem. Soc.* **143** (1996) 825.

Received 6 April 2004
and accepted 25 May 2005